Flexible Ultra-resolution Subdermal EEG Probes

Zabir Ahmed, Jay Reddy, Kaustubh Deshpande, Ashwati Krishnan, Praveen Venkatesh, Shawn Kelly,
Pulkit Grover and Maysamreza Chamanzar
Department of Electrical and Computer Engineering, Carnegie Mellon University, Pittsburgh, USA
email: mchamanzar@cmu.edu

Abstract*—Scalp Electroencephalogram (EEG) is a popular, noninvasive method to record neural activity, commonly used in the clinical setting as a gold-standard for diagnosing many disorders, including epilepsy. The spatial resolution of scalp EEG is of critical concern for targeting surgical interventions and resultant patient outcomes. However, high-resolution spatial information is filtered and obscured by noise as electrical signals propagate through layers of tissue. We present a novel paradigm of high-density subdermal EEG arrays, capable of being implanted under the scalp to increase spatial resolution of EEG recordings while minimizing invasiveness compared to traditional implantable recording electrode arrays such as electrocorticography (ECoG) surface grids. In addition, our device can be chronically implanted, as opposed to traditional scalp EEG electrodes that need to be removed periodically for re-application of conductive electrode gel. We demonstrate the design, fabrication and electrical characterization of high-density subdermal EEG arrays realized in Parylene C polymer platform using an optimized microfabrication process. Devices are realized in a range of electrode diameters (200 microns - 1000 microns) and pitch (1 mm - 3.5 mm), to study the effects of electrode size and spacing on the spatial frequency content and redundancy of recorded neural signals. Electrochemical Impedance Spectroscopy (EIS) measurements, show an impedance of <10 kΩ (for 600 micron diameter) at 1 kHz. These high-density subdermal EEG probes will be used to validate our theoretical models of sampling and reconstructing neural activity from electric potentials.

I. Introduction

Scalp Electroencephalography (EEG) is a widely used non-invasive modality to monitor the electrical activity of the brain for diagnosis of medical conditions ranging from sleep disorders and epilepsy to stroke and traumatic brain injury [1], [2]. When compared with invasive modalities such as Electrocorticography (ECoG) and penetrating depth electrodes, traditional scalp EEG has the advantage of being non-invasive, and therefore of minimizing the risk of infection resulting from surgery. While volume conduction through the skull and the scalp significantly reduces the spatial resolution of scalp EEG, this can be partially compensated for by increasing the density of EEG electrodes [3], [4]. However, currently available scalp EEG systems are not suitable for chronic, long-term measurements (needed, for instance, during the diagnosis of epilepsy, where the timings of seizures are unpredictable) because the conductive gels used in these systems dry out within a few hours of use. We propose subdermal EEG as a minimally-invasive alternative to scalp EEG, which has significantly higher spatial resolution and is suitable for long-term monitoring.

Subdermal "needle" electrodes are commonly used in order to reduce the recording impedance from skin and hair and for chronic placement [5]–[8]. However, existing devices, including some recent advances [9], lack the density needed to maximize spatial resolution. A minimally invasive, high resolution device would be clinically applicable, e.g., for epileptic focus localization and for detecting spatially subtle signals in the brain.

Recent work has shown theoretically [3] and experimentally [4] that ultra high-density scalp EEG (having an inter-electrode separation of ~1 cm or less) can provide a high spatial-resolution view of brain activity. To derive maximum spatial resolution from the use of *subdermally* placed probes, which suffer reduced signal attenuation compared to scalp EEG, an even denser subdermal electrode array is necessary (discussed in Section II). Existing low-density subdermal EEG electrodes [10] are not well-suited for examining the fundamental spatial-resolution limits of this architecture. Therefore, we present novel, microfabricated, high-density subdermal EEG arrays to characterize these limits using established benchmarks [11].

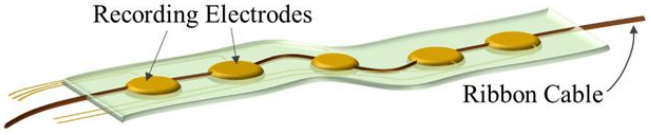

Fig. 1 Schematic of our microfabricated high density subdermal EEG electrode array realized on a flexible biocompatible polymer substrate.

II. Information-theoretic Motivation

EEG records electric potentials, on the scalp or under the dermis, generated as a result of neural activity within the brain [12]. The electric fields produced by neurons propagate through poorly-conductive skull and thick layers of scalp, and in the process, suffer from spatial low-pass filtering. This filtering effect has traditionally been analyzed using a concentric-spheres model [12] of the brain, skull and scalp, for which the transfer function can be analytically derived [3] (Fig. 2).

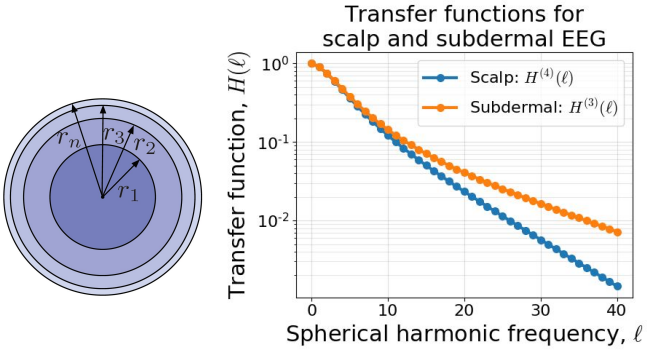

Fig. 2 (Left) Schematic of a spherical head model with four layers, consisting of brain (r<8 cm), cerebrospinal fluid (CSF; 8 cm<r<8.2 cm), skull (8.2 cm<r<8.7 cm) and scalp (8.7 cm<r<9 cm). (Right) Theoretical transfer function vs. spatial frequency showing the low-pass filtering effect of volume conduction, calculated by analytically solving Poisson's equation in the quasistatic regime. At higher spatial frequencies, scalp EEG suffers much greater attenuation than subdermal EEG.

978-1-5386-3603-9/18/$31.00 ©2018 IEEE

A fundamental question is whether there are benefits in sampling closer to the skull than is done through scalp EEG. To understand this question better, we plotted the transfer function of the spatial low-pass filter against distance from the brain's surface in a 4-sphere head model (Fig. 3). Using this figure, we can compare relative signal amplitudes at different spatial frequencies (measured in the spherical harmonic basis), and at different depths from the scalp. At high spatial frequencies, e.g. *l=40*, (corresponding to an average inter-electrode distance of 0.5 cm on the scalp; refer Fig. 10a of [3]), the scalp alone attenuates the signal by a factor of ~16. Thus we see that although the signal attenuation is predominantly caused by the skull, at sufficiently high spatial frequencies, the attenuation caused by the scalp is also significant. It is these high spatial frequencies that carry high spatial resolution information, so their attenuation results in a loss of spatial resolution. To image the brain with higher spatial resolution, therefore, it is helpful to (i) sample higher spatial frequencies using sufficiently dense electrode arrays closer to the skull, and (ii) record these high spatial frequencies with high SNR.

While the importance of points (i) and (ii) stated above has been argued theoretically [3], [13], [14], experimental validation of the same has remained elusive, largely due to the absence of devices using which such claims can be tested. The flexible, ultra-resolution subdermal EEG probes discussed in this paper will enable us to validate our theoretical understanding of sampling electric potentials and reconstructing neural activity within the brain.

Furthermore, points (i) and (ii) above share a trade-off in terms of electrode size: arrays of higher density will require smaller electrodes, but smaller electrodes will have larger impedance and therefore, lower SNR. In practice, a well-designed subdermal EEG system will seek to find the optimum electrode size for maximizing spatial resolution, while maintaining a reasonably high SNR. To characterize this trade-off, we designed and implemented several variants of the proposed probes with differing electrode size and spacing (see Sections III and V) .

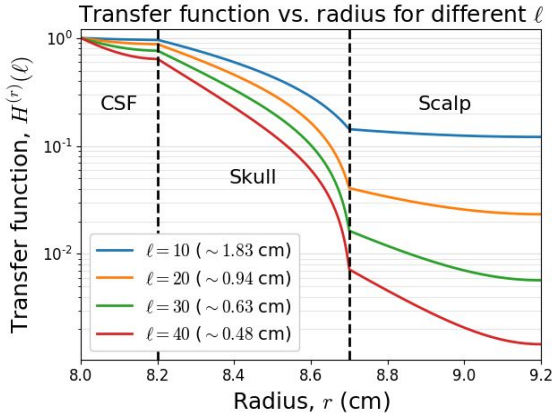

Fig. 3 Analytically derived transfer function for a 4-sphere head model, showing attenuation of potential with distance from the brain's surface. Attenuation is measured relative to the signal amplitude on the cortex. Different curves indicate different spatial frequencies. Higher 'l' corresponds to higher spatial frequency. The average inter-electrode distance required to sample each frequency (using scalp EEG) is shown in parentheses.

III. Design of Subdermal EEG

The subdermal EEG probes are fabricated in a Parylene C polymer platform, which is preferred to other material platforms (SU-8, Polyimide, PDMS) for its excellent mechanical strength and flexibility, barrier properties, biocompatibility, and conformal, room temperature deposition process [15]. Although polymer probes carry concerns of implantation failure due to buckling, techniques to temporarily stiffen the cable using bioresorbable coatings or a rigid implantation shuttle have been developed [16]. Our probe consists of a linear array of 30 circular electrodes uniformly distributed along its length. Multiple probe variants were fabricated, with electrode diameter ranging from 200 µm to 1 mm and pitch varying from 1 mm to 3.5 mm, forming a total device length of 5 to 8 cm. At the backend of the device, a high density bondpad array with 250 µm pitch is used to interface with recording devices. The subdermal EEGs contain a 1 cm cable separating the recording electrode arrays from the backend interface to allow for ease of assembly and experimental setup. Fig. 4 shows a released subdermal EEG probe. Total device thickness is 10 µm, allowing for a highly flexible and minimally invasive neural interface. These devices, with a high number of channels on a biocompatible, flexible polymer platform, can potentially record long term EEG signals with high signal fidelity and spatial resolution.

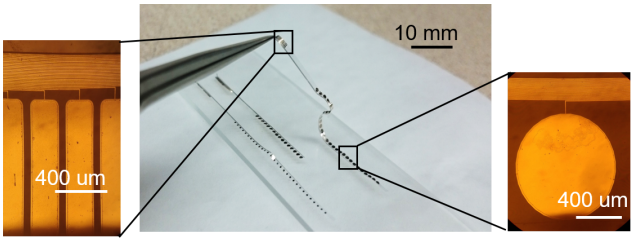

Fig. 4 (Bottom) Photograph of fabricated subdermal EEG probes with inset microscopy images of (top left) dense backend interconnects and (top right) large recording electrodes.

IV. Fabrication of Subdermal EEG Probes

We have developed an optimized fabrication process for Parylene-based subdermal EEG probes. The process flow is graphically illustrated in Fig. 5.

Fabrication is performed on 4 inch silicon wafers. A 5 µm layer of Parylene C is deposited as the device substrate (SCS Labcoter - 2). Metal traces are lithographically defined on Parylene C via a lift-off process (LOR 3A, S1805 Photoresist and CD-26 Developer). Metal traces are deposited using e-beam evaporation (Kurt J. Lesker PVD 75 Electron Beam Evaporator). The metal stack consists of 5 nm of Pt, 120 nm of Au, and 5 nm of Pt. The Pt serves as an adhesion layer to Parylene. Lift-off is performed by soaking the sample for 2 hours in 60° C heated Microposit Remover 1165 (Microchem GMBH). A 5 µm upper insulation layer of Parylene C is deposited, which is then patterned to expose the electrode sites and bondpads, as well as to define the probe outlines. Parylene is patterned using O_2 reactive ion etching (RIE) with TRION Phantom II RIE. A 100 nm evaporated Cr hardmask is used during etching (Kurt J. Lesker PVD 75 Electron Beam Evaporator) to overcome the poor selectivity of Parylene C to photoresist. The thin film stress of deposited Cr was controlled to prevent cracking of

Parylene underneath. The hardmask is patterned lithographically (AZ 4210) and wet etched in Cr 1020 Etchant (Microchem GMBH). After RIE etching, the Cr hardmask is stripped using Cr Etchant. Devices are released by soaking the wafer for 15- 30 minutes in Micro-90 Microsoap, which is commonly used as a release agent for Parylene [17]. After release, the devices are thoroughly washed with DI water to remove any residual Microsoap.

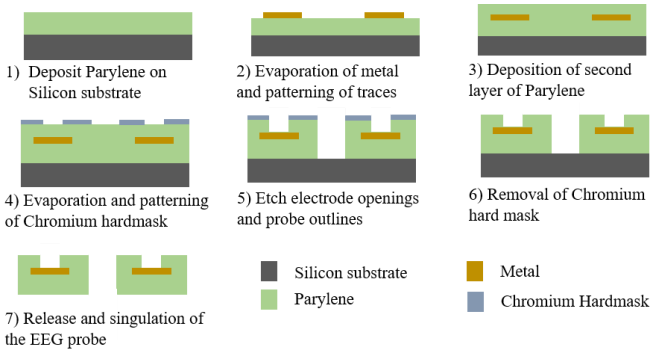

Fig 5. Microfabrication process flow for subdermal EEG.

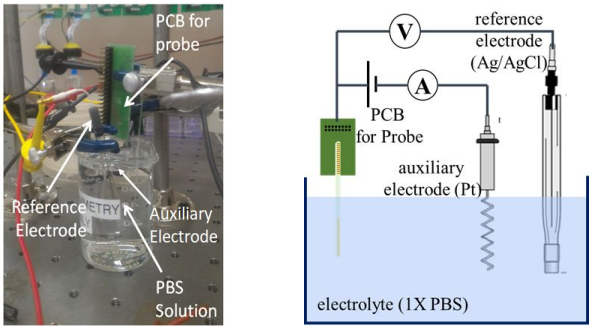

Fig 6. Electrochemical Impedance Spectroscopy characterization setup showing the microfabricated released subdermal EEG probe attached to a printed circuit board (PCB), reference and auxiliary electrode in 1X PBS solution

V. Results: Electrochemical Impedance Measurement

Electrochemical Impedance Spectroscopy (EIS) was used to characterize the electrochemical performance of the probes (Fig. 6). Measurements were performed in PBS (Phosphate Buffered Saline) solution with PGSTAT302N potentiostat (Metrohm Autolab, Netherlands) with a 3-electrode configuration operating in potentiostatic mode. The counter/auxiliary electrode was a platinum wire electrode (MW-1032, BASI Inc) and the reference electrode was Ag/AgCl electrode (MF-2052, BASI Inc).

Impedance measurements were conducted over the frequency range of interest for neural recording: 0.1 Hz - 10 kHz using a 50 mV root-mean-square sinusoidal signal at open circuit potential. Fig. 7 shows magnitude and phase measurements of the EIS from subdermal EEG devices with 600 µm (a and b) and 800 µm (c and d) diameter electrode sites.

The average impedance magnitudes of the functional channels at 1 kHz were found to be 7 kΩ and 4 kΩ for 600 µm and 800 µm diameter, respectively. These values are consistent with previously reported results in literature for neural probes with similar electrode sizes [18].

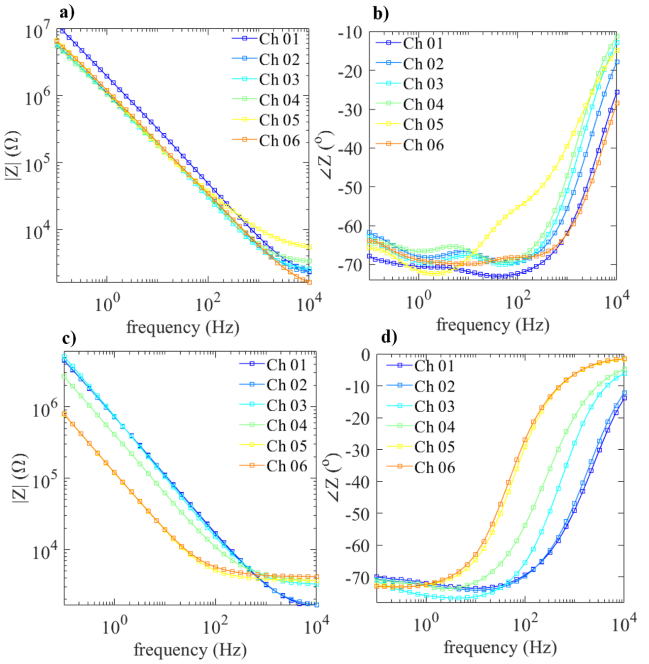

Fig. 7 EIS measurement plots of different channels of subdermal EEG probes with 600 µm (a, b) and 800 µm (c,d) diameter electrodes. a) and c) show the impedance magnitude, b) and d) show the phase over 0.1 Hz- 10 kHz. At 1 kHz, average impedances are ~ 7 kΩ. and ~4 kΩ for 600 µm and 800 µm diameter electrodes, respectively.

As discussed in Section II, to achieve a high spatial resolution, we would prefer small electrode sizes, which result in higher impedances and consequently lower SNR. To break this trade-off, we can reduce the impedance of our electrodes by an order of magnitude through post-fabrication modification of the electrode sites, without changing the electrode sizes by electrochemical deposition of PEDOT:PSS on the electrodes. This is an effective means of improving the electrode-electrolyte interface impedance, as demonstrated in our previous work [19].

VI. Results: Accelerated Lifetime Testing

Long-term probe stability was characterized via accelerated lifetime testing (ALT), performed in 70 ºC heated PBS with EIS measurements performed at the same temperature at intervals shown in Fig 8. Accelerated lifetime testing is characterized by

$$t_{37} = t_r \times Q_{10}^{\frac{(T-37)}{10}},$$

where t_{37} is the simulated age; t_r is the time aged at temperature T; and Q_{10} is the temperature coefficient typically taken as 2 for polymers, yielding 10 simulated days in our test [20], [21], which is comparable to the typical monitoring time (1-2 weeks) for epilepsy patients. Channel failure was characterized by a sudden increase in impedance (after 24 hours), indicating an open channel caused by a broken trace in the subdermal EEG cable or corrosion of the recording electrode surface. The thickness of the Parylene layers and the traces can be increased to make these subdermal probes more resistant to mechanical failure, and PEDOT:PSS surface coating should increase the electrode corrosion resistance. A typical channel showed very stable impedance characteristics for the first 24 hours (Fig. 8). These results suggest that our probes provide a robust

electrochemical recording interface, suitable for long-term recordings.

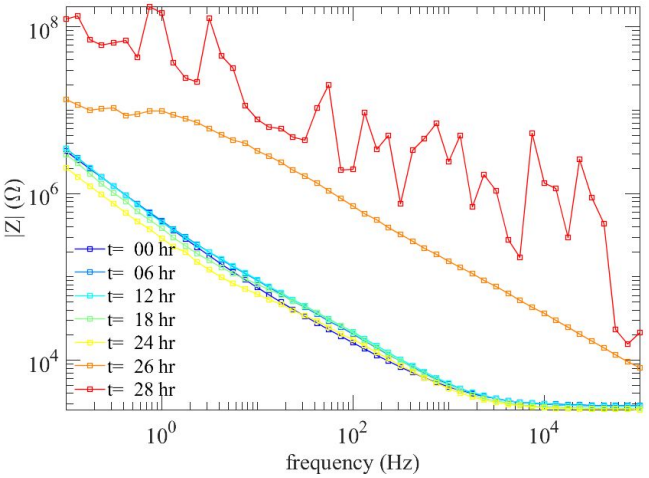

Fig. 8 ALT measurement plots of a subdermal EEG probe channel aged at 70°C at intervals denoted in the legend. Channel impedance is shown to be very stable to the point of failure after 24 hours (corresponding to 10 simulated days).

VII. Conclusions and Future Work

The presented novel microfabricated high-density subdermal EEG probes can be used for chronic long term recording of neural activity. Therefore, these probes are ideal for ambulatory monitoring, especially in situations requiring fixed-electrode positions for source localization, for example to detect seizure foci in epileptic patients. As opposed to ECoG and penetrating depth electrodes, where the neural probes traverse through the skull, increasing the risk of infection and trauma to the brain tissue, our subdermal EEG probes can be implanted under the skin in the scalp using a minimally invasive procedure, albeit at the cost of lowering signal resolution.

We have designed adaptor electronic boards to connect the neural probes to an external recording system (RHD 2132, Intan Inc.) and optimized the packaging of these flexible probes to the adaptor board using a wire bonding technique. Glob top epoxy will be used to encapsulate the wire bonds to ensure the insulation and mechanical stability of the bonds and the probe itself. We will carry out in-vivo experiments on rodents and primates to test and validate the efficacy of the subdermal EEG probes presented here, and will compare their performance to traditional scalp EEG recordings. We expect a higher SNR in subdermal EEG recordings as a result of reduced signal attenuation and dispersion under the skin. Being integrated in the scalp, we also expect subdermal EEG to be relatively immune to artifacts caused by movement of electrodes commonly seen in scalp EEG, further improving SNR. We will also characterize the trade-off between the electrode density and SNR. We will also evaluate the effectiveness of electrochemical deposition of PEDOT conductive polymer on exposed electrodes to reduce the impedance and enhance the signal quality.

In the future, we can envision integrating wireless power and data transceiver chips to the probe backend so that the subdermal probes can be completely embedded and sealed under the skin and controlled using an external transponder, fully realizing the potential of these devices for chronic, untethered recording.

References

[1] A. T. Tzallas, M. G. Tsipouras, and D. I. Fotiadis, "Epileptic Seizure Detection in EEGs Using Time–Frequency Analysis," *IEEE Trans. Inf. Technol. Biomed.*, vol. 13, no. 5, pp. 703–710, 2009.

[2] P. Vespa, "Continuous EEG monitoring for the detection of seizures in traumatic brain injury, infarction, and intracerebral hemorrhage: 'to detect and protect,'" *J. Clin. Neurophysiol.*, vol. 22, no. 2, pp. 99–106, Apr. 2005.

[3] P. Grover and P. Venkatesh, "An Information-Theoretic View of EEG Sensing," *Proc. IEEE*, vol. 105, no. 2, pp. 367–384, 2017.

[4] A. K. Robinson, P. Venkatesh, M. J. Boring, M. J. Tarr, P. Grover, and M. Behrmann, "Very high density EEG elucidates spatiotemporal aspects of early visual processing," *Sci. Rep.*, vol. 7, no. 1, p. 16248, Nov. 2017.

[5] Y. B. Benovitski *et al.*, "Ring and peg electrodes for minimally-Invasive and long-term sub-scalp EEG recordings," *Epilepsy Res.*, vol. 135, pp. 29–37, 2017.

[6] G. B. Young, J. R. Ives, M. G. Chapman, and S. M. Mirsattari, "A comparison of subdermal wire electrodes with collodion-applied disk electrodes in long-term EEG recordings in ICU," *Clin. Neurophysiol.*, vol. 117, no. 6, pp. 1376–1379, Jun. 2006.

[7] J. Väisänen, K. Wendel, G. Seemann, J. Malmivuo, and J. Hyttinen, "Sensitivities of Bipolar Subcutaneous and Cortical EEG Leads," in *IFMBE Proceedings*, 2009, pp. 267–270.

[8] J. Duun-Henriksen *et al.*, "EEG Signal Quality of a Subcutaneous Recording System Compared to Standard Surface Electrodes," *Journal of Sensors*, vol. 2015, pp. 1–9, 2015.

[9] B. G. Do Valle, "Long-Term, Subdermal Implantable EEG Recording and Seizure Detection," Ph.D., Massechusetts Institute of Technology, 2016.

[10] B. G. Do Valle, S. S. Cash, and C. G. Sodini, "Low-Power, 8-Channel EEG Recorder and Seizure Detector ASIC for a Subdermal Implantable System," *IEEE Trans. Biomed. Circuits Syst.*, Apr. 2016.

[11] A. S. Oliveira, B. R. Schlink, W. D. Hairston, P. König, and D. P. Ferris, "Proposing Metrics for Benchmarking Novel EEG Technologies Towards Real-World Measurements," *Front. Hum. Neurosci.*, vol. 10, p. 188, May 2016.

[12] P. L. Nunez and R. Srinivasan, *Electric Fields of the Brain: The Neurophysics of EEG*. Oxford University Press, USA, 2006.

[13] P. Grover, "Fundamental limits on source-localization accuracy of EEG-based neural sensing," in *2016 IEEE International Symposium on Information Theory (ISIT)*, 2016.

[14] P. Venkatesh and P. Grover, "Lower bounds on the minimax risk for the source localization problem," in *2017 IEEE International Symposium on Information Theory (ISIT)*, 2017.

[15] B. J. Kim and E. Meng, "Micromachining of Parylene C for bioMEMS," *Polym. Adv. Technol.*, vol. 27, no. 5, pp. 564–576, 2015.

[16] A. Weltman, J. Yoo, and E. Meng, "Flexible, Penetrating Brain Probes Enabled by Advances in Polymer Microfabrication," *Micromachines*, vol. 7, no. 10, p. 180, 2016.

[17] B. J. Kim and E. Meng, "Micromachining of Parylene C for bioMEMS," *Polym. Adv. Technol.*, vol. 27, no. 5, pp. 564–576, 2015.

[18] A. K. Ahuja, M. R. Behrend, J. J. Whalen, M. S. Humayun, and J. D. Weiland, "The dependence of spectral impedance on disc microelectrode radius," *IEEE Trans. Biomed. Eng.*, vol. 55, no. 4, pp. 1457–1460, Apr. 2008.

[19] M. Chamanzar, D. J. Denman, T. J. Blanche, and M. M. Maharbiz, "Ultracompact optoflex neural probes for high-resolution electrophysiology and optogenetic stimulation," in *2015 28th IEEE International Conference on Micro Electro Mechanical Systems (MEMS)*, 2015.

[20] S. A. Hara *et al.*, "Pre-implantation electrochemical characterization of a Parylene C sheath microelectrode array probe," *Conf. Proc. IEEE Eng. Med. Biol. Soc.*, vol. 2012, pp. 5126–5129, 2012.

[21] D. W. L. Hukins, A. Mahomed, and S. N. Kukureka, "Accelerated aging for testing polymeric biomaterials and medical devices," *Med. Eng. Phys.*, vol. 30, no. 10, pp. 1270–1274, 2008.